©SNAK, 2015

Int. J. Nav. Archit. Ocean Eng. (2015) 7:805~816
http://dx.doi.org/10.1515/ijnaoe-2015-0057
pISSN: 2092-6782, eISSN: 2092-6790

Welding deformation analysis based on improved equivalent strain method to cover external constraint during cooling stage

Tae-Jun Kim[1], Beom-Seon Jang[2] and Sung-Wook Kang[2]

[1]*Hyundai Heavy Industries Co., Ltd., Ulsan, Korea*
[2]*RIMSE, Dept. of Naval Architecture and Ocean Engineering, Seoul National University, Seoul, Korea*

Received 24 July 2014, Revised 14 January 2015, Accepted 13 March 2015

ABSTRACT: *In the present study, external restraints imposed normal to the plate during the cooling stage were determined to be effective for reduction of the angular distortion of butt-welded or fillet-welded plate. A welding analysis model under external force during the cooling stage was idealized as a prismatic member subjected to pure bending. The external restraint was represented by vertical force on both sides of the work piece and bending stress forms in the transverse direction. The additional bending stress distribution across the plate thickness was reflected in the improved inherent strain model, and a set of inherent strain charts with different levels of bending stress were newly calculated. From an elastic linear FE analysis using the inherent strain values taken from the chart and comparing them with those from a 3D thermal elasto-plastic FE analysis, welding deformation can be calculated.*

KEY WORDS: Welding deformation; Inherent strain; FE analysis; Equivalent strain method; External constraint.

INTRODUCTION

In shipyards, a vessel is constructed by assembling a lot of blocks which are fabricated by assembling respective sub-blocks again. Welding inevitably induces distortion of a block, and this is accumulated during the sequential fabrication process. As the block erection step accounts for about one-third of the whole shipbuilding process, the accuracy of a block in terms of shape and dimension has a critical influence on overall efficiency of production in the shipyard. The welding distortions reduce the fabrication accuracy of ship-hull blocks, and decrease productivity, due to the amount of correction work that is required. To increase the precision of fabrication, the welding distortion and the exact distortion margin at every fabrication stage should be estimated in order to meet the allowable tolerances of ship-hull blocks.

Prediction and control of welding distortions at the design stage, an essential task of shipyards, ensures both high quality and high productivity (Jang, 2007). The most widely utilized method of this type is the thermal Elasto-Plastic Analysis (EPA) method, which delivers relatively accurate results. However, due to the consideration of complicated nonlinearity of material property, it requires long computational time. Thus, the inherent strain method has been developed and improved for an efficient prediction of the welding deformation and welding residual stress (Kim, 2006; Lee, 2002; Kim, 2010).

During welding process, vertical deformation is suppressed vertically on flat work piece in order to reduce the residual welding deformation. This study investigates the effect of the vertical restraints on the residual deformation first and proposes

Corresponding author: *Beom-Seon Jang*, e-mail: *seanjang@snu.ac.kr*

an efficient method for a prediction of welding deformation and residual stress subject to the vertical restraints. This is enabled by incorporating the vertical restraint effect into the inherent strain method as tensile or compressive stress. This proposed method is to be verified in various examples comparing the results with thermal-elasto plastic analysis.

DEFINITION OF INHERENT STRAIN

Inherent strain is defined as follows. Initially, there is a material object that has no stress distribution. When it is under stress, stress acting on a material element is accompanied by strain. Even once the stress is released by cutting out a small piece of material, residual and irrecoverable strain might still exist. This strain is regarded as the inherent strain.

Inherent strain can be further explained by means of the three material states shown in Fig. 1 (Lee, 1999). The initial state has no stress distribution inside (Fig. 1(a)); the material experiences a stressed condition caused by phenomena such as thermal strain (Fig. 1(b)); the stress is partially released by cutting out a small piece of the material (Fig. 1 (c)).

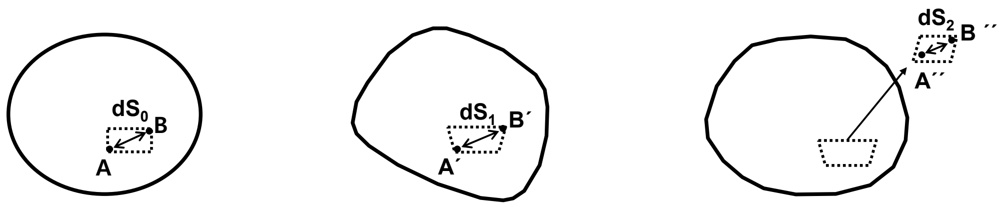

(a) Initial state (stress free). (b) Stressed state. (c) Stress released state.

Fig. 1 Definition of inherent strain.

Based on the above definition, the inherent strain (ε^*) is expressed, by subtracting the elastic strain from the total strain, as

$$\varepsilon^* = \frac{\overline{A''B''} - \overline{AB}}{\overline{AB}} = \frac{dS_2 - dS_0}{dS_0} \tag{1}$$

The total strain can be divided into the thermal (th), plastic (p), and elastic (e) strains,

$$\varepsilon = \varepsilon^{th} + \varepsilon^{p} + \varepsilon^{e} \tag{2}$$

After the welding process, the thermal strain becomes zero, and the inherent strain is the same as the plastic strain (Kim, 2006):

$$\varepsilon^* = \varepsilon - \varepsilon^{e} = \varepsilon^{p} \tag{3}$$

IMPROVED EQUIVALENT STRAIN METHOD CONSIDERING TEMPERATURE DISTRIBUTION

Kim et al. (2014) suggested an Improved Equivalent Strain Method (Improved ESM) considering the temperature distribution. The inherent strain model, a solid-spring model, used for generating inherent strain chart is briefly explained here. When a small element in the middle of entire model expands or shrinks by the temperature difference, its deformation is restrained by elements surrounded along the direction of deformation rather than those perpendicularly attached to the direction as shown in Figs. 2 and 3 shows a 2D biaxial model where springs resisting against the deformation of the center element are relocated to represent the above-mentioned phenomenon. Fig. 4 shows 3D tri-axial restraint model. The process of determining the elastic modulus of the periphery to induce the equivalent restraint is described by Kim et al. (2014). A solid-spring model is considered to be axially symmetric. One of the two faces normal to each axis is fixed, and the other is allowed to move freely along the axis. This boundary condition prevents a rigid body motion, without disturbing the intended structural behavior. The boundary condition adopted in this analysis is depicted in Fig. 5.

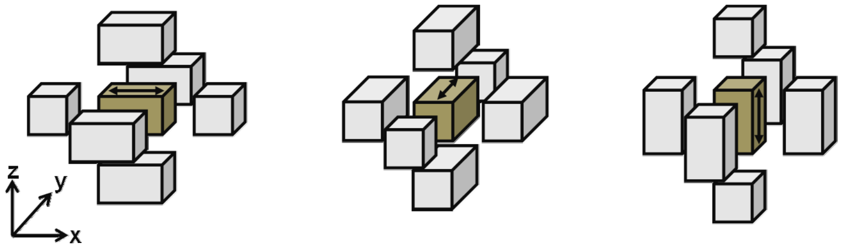

Fig. 2 Restraining elements for each load direction.

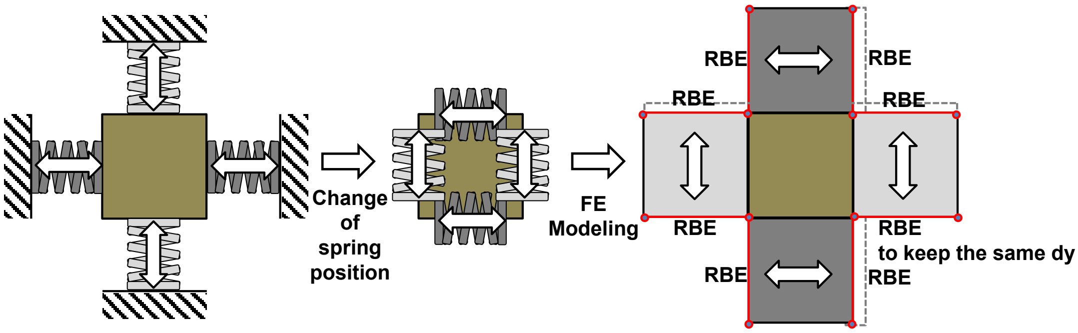

Fig. 3 Biaxial restraints model.

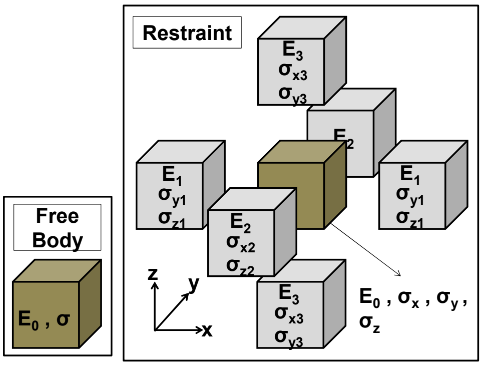

Fig. 4 Disassembled view of tri-axial restraints model.

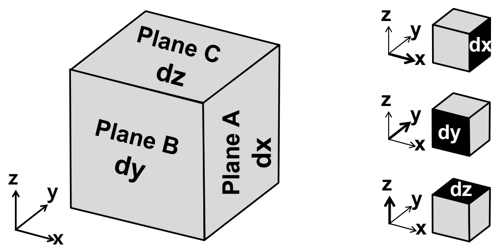

Fig. 5 Boundary condition on core element.

The degree of restraint of the welding model is expressed by the ratio of a core-element strain under restraint (ε', Fig. 6(b)) at the periphery to that without restraint (ε_0, Fig. 6(a)). It varies due to temperature changes in the welding process, as shown in Fig. 7. Different temperature distribution along the three axes can cause a difference in the three axial restraints, and thereby can induce residual plastic strain. Thus, transverse temperature gradient (TG_x) and through-thickness temperature gradient (TG_z) are newly defined as factors affecting the inherent strain as well as the maximum welding temperature. Details are described by Kim et al. (2014).

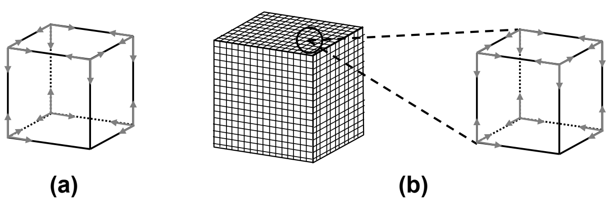

Fig. 6 Unit load method of welding model.

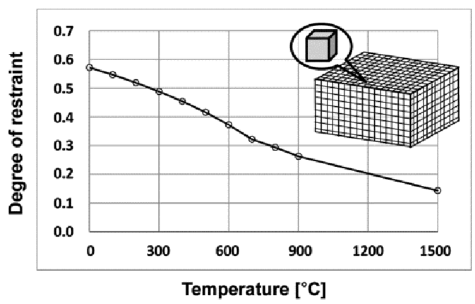

Fig. 7 Temperature-degree of restraint relation.

A series of EPA considering temperature dependent material properties (Lee, 1995) is performed varying maximum welding temperature, TG_x and TG_z. An inherent strain chart for mild steel is generated as Figs. 8 and 9. Fig. 8 displays the overlapped strain charts for maximum temperatures ranging from 600 °C to 1500 °C with 100 °C increment. The x-, y-, and z-axes represent transverse temperature gradient (TG_x), through-thickness temperature gradient (TG_z), and the inherent strain, respectively. Fig. 9 shows the inherent-strain maximum temperature curve at a TG_z of 0.4. TG represents the relative magnitude of the temperature gradient between the core element and the periphery element.

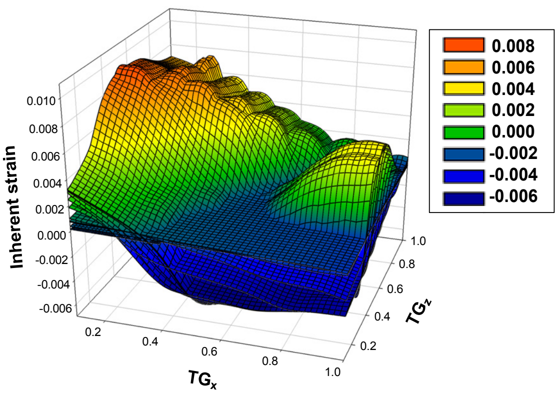

Fig. 8 Inherent strain chart.

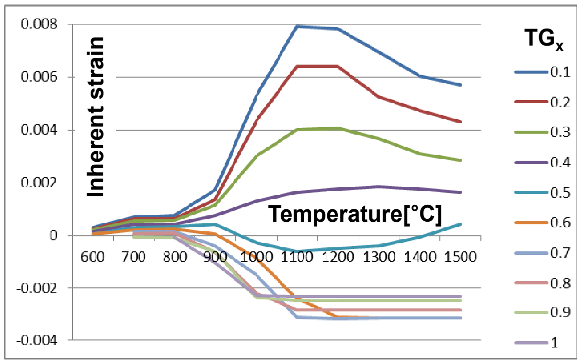

Fig. 9 Inherent strain curve at TG_z=0.4.

THE EFFECT OF EXTERNAL CONSTRAINT ON THE WELDING DEFORMATION

This section begins with a mechanism how welding deformation forms during butt welding of a plate. During the butt welding process, an external constraint can be imposed perpendicular to the side of the plate in order to reduce its angular distortion. At which stage (heating, cooling or both stages) should the restraint be applied to be effective to the reduction of angular distortion. This is examined by a case study. Then, the restraint is represented as a bending moment along the welding line and the assumption is validated through a case study.

Residual welding deformation in butt welding

Basically, heat induces a thermal stress and strain, as shown in Fig. 10(a). Here, only one side of the plate is heated; so, the heated region expands and creates a reaction force. This reaction makes the heated area convex as Fig. 10(b). After this, the heated area is cooled by water or air, which induces shrinkage of the expanded region and generates a contraction force like Fig. 10(c). Finally, due to the shrinkage, angular distortion remains (Fig. 10(d)). The angular distortion is caused by non-uniform temperature gradient across plate thickness due to the one-sided heating, which results in different amounts of plate expansion and shrinkage through the thickness direction at the heated local area.

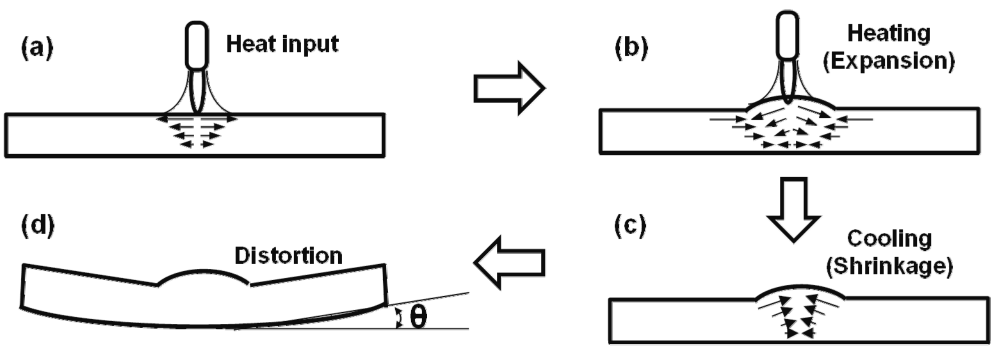

Fig. 10 Welding deformation algorithm (Radaj et al., 2003).

Effect of external constraint during welding stages

If an external constraint is imposed perpendicularly on flat work piece during its welding, it is known to reduce the final welding deformation. Regarding the application of the constraints, three alternatives are available; restrained during both heating and cooling stages, heating stage only, and cooling stage only. This section investigates which one results in the least welding deformation through a case study. A 2D FE model using plane strain elements of which half width and thickness 300 *mm* and 10 *mm*, respectively is built as shown in Fig. 11(a). As the model is symmetric, a half model is built with x-axis symmetric boundary condition along the center line and the welding heat is applied at the center point.

The vertical restraint (z-direction) is imposed at the point 100 *mm* located from the center welding point as well as the center point as shown in Fig. 11(b). Four different cases are defined depending on the stages under the vertical restraint as listed in Table 1. EPA is performed for the four cases and resultant vertical residual deformations at the edge of the plate are listed in Table 1. Fig. 12 depicts the vertical deformation plots.

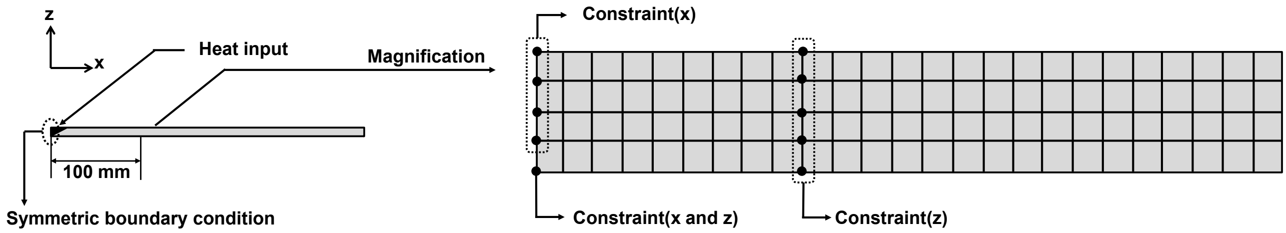

(a) Half model. (b) Vertical restraint at weld point and 100 *mm* from welding point.

Fig. 11 2D FE model and vertical restraint point.

Table 1 Maximum deformation in z direction.

	Stage under constraint		Max. deform. (*mm*)
	Heating	Cooling	
CASE I	X	X	0.724
CASE II	O	O	1.051
CASE III	O	X	1.751
CASE IV	X	O	0.467

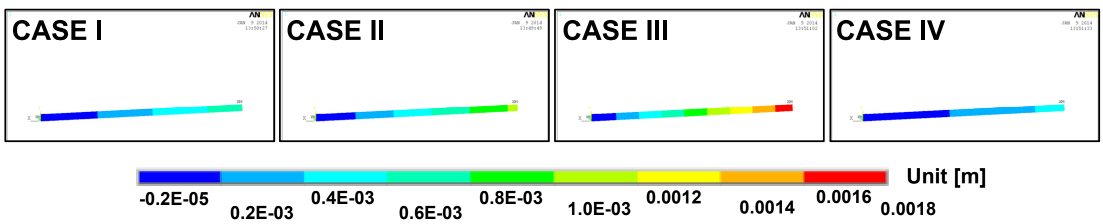

Fig. 12 Deformation in z direction.

As expected, the suppression of vertical deformation during only cooling stage (CASE IV) leads to the least deformation and less than the case without any constraints (CASE I). On the other hand, the residual deformations of CASE II and CASE III are larger than CASE I. This result is meaningful since it can improve welding accuracy by reducing the welding distortion with an appropriate restraint. It would be more beneficial, if it could be predicted what restraint point is most effective to the reduction of welding deformation and how much the deformation remains. An easy prediction to replace than time-consuming thermal elasto-plastic FE analysis is necessary for an application to actual construction process. This paper aims at proposing an efficient method to estimate the welding deformation under vertical restraints based on the inherent strain method.

Simplification of welding analysis considering external constraint during cooling

In actual welding process, a jig is widely used to mitigate the vertical deformation. The vertical restraint is represented by a reaction force at the jig location and the reaction force may change during the cooling process. However, the constraint is hard to be directly realized in the inherent strain model because it is a micro model and there is no way to reflect the vertical restraint imposed on the entire model as it is into the micro model. The changing reaction force is also difficult to be incorporated into the simplified inherent strain chart. Thus, as the first step, this research simply assumes a certain weight is loaded at the jig location and focuses on the effect of constant force on the inherent strain and the resultant welding deformation instead of the vertical restraint itself. How to treat the varying reaction force will be investigated as the next step. The vertical restraint during cooling stage can be modeled as normal forces P applied at distance of 'a' from the weld line as depicted in Fig. 13. The moment acting on the welded region by the external normal force P, M, is represented as M=Pa.

It is also assumed that this welding analysis model is a prismatic member subjected to pure bending; therefore, external normal force P can be represented by linearly distributed x-directional bending stress as shown in Fig. 14.

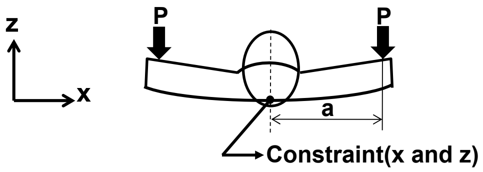

Fig. 13 Analysis model subjected to external load.

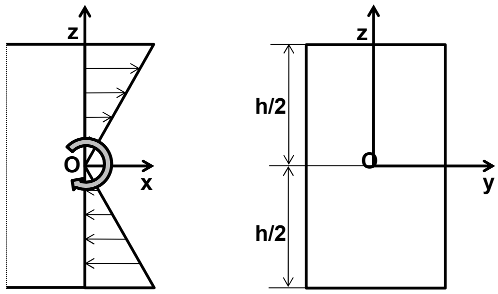

Fig. 14 Cross-section view of simplified concept model.

Specifying that the normal stress at any distance z from the neutral axis is obtained from the beam theory

$$\sigma_x = -\frac{Mz}{I} \tag{4}$$

The welding analysis under external normal force during cooling is idealized as a problem under compressive or tensile stress in the x direction and the stress depends on the location of constraint, the magnitude of constraint, and the applied location in the thickness direction.

Validation of assumption

In this section, EPA is performed to verify whether it is valid to replace the normal external constraint force P by the moment, M. Three different cases of normal force are assumed as shown in Fig. 15. Each case has different force magnitude and location, but has the same bending moment, 0.3 $kN{\cdot}m$, at the center point. The same 2D FE model using plane strain element as Fig. 11 is built and EPA is performed for three load cases. The external loads are applied to the plate during only cooling stage. The resultant vertical welding deformations show a good agreement as depicted in Fig. 15.

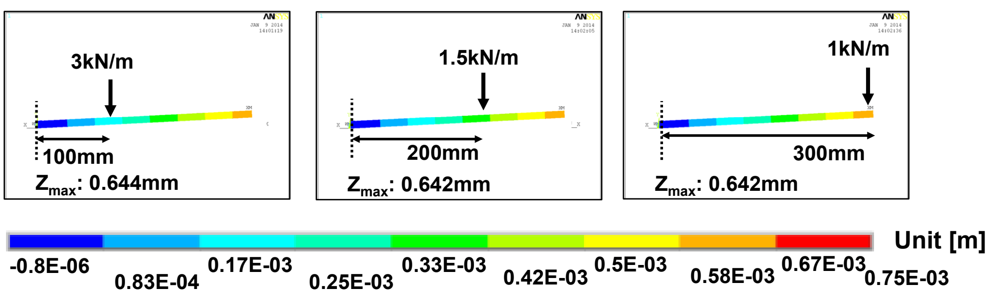

Fig. 15 Analysis results of model of external force acting during cooling.

INHERENT STRAIN MODEL WITH EXTERNAL CONSTRAINTS

This section describes how to incorporate the effect of external vertical restraints in butt welding into the inherent strain model and the inherent strain charts obtained from the EPA for the solid-spring model. It is also explained how the angular distortion can be reduced when applying the method to actual butt welding.

The inherent strain model and the procedure to obtain the inherent strain are basically identical to those of the Improved ESM, except that additional compressive or tensile stress in the x direction is applied in cooling stage as illustrated in Fig. 16. EPA is performed for the heat applied to the center element. Details of the Improved ESM can be referred to Kim et al. (2014).

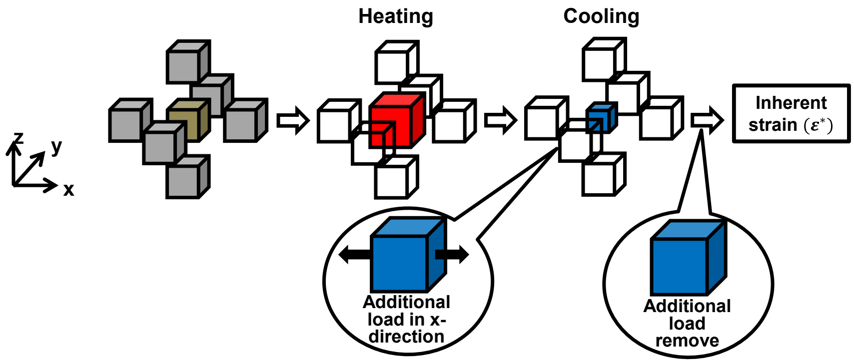

Fig. 16 Inherent strain model considering external load during cooling stage.

A series of thermal-elasto plastic analysis is performed for the inherent strain model varying, maximum welding temperature, transverse temperate gradient (TG_x), through-thickness temperate gradient (TG_z), and the axial stress(σ_x) in cooling stage. Fig. 17 displays the improved inherent strain charts for three maximum welding temperatures. As the tensile axial stress increases, the tensile residual plastic strain also grows. It becomes remarkable when the maximum heating temperature becomes higher.

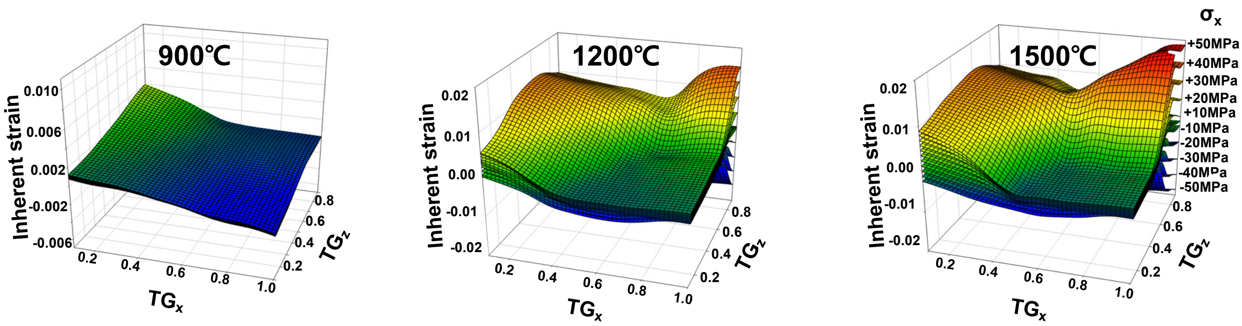

Fig. 17 Inherent strain charts considering external load during cooling.

In the inherent strain model of Fig. 16, tensile stress during the cooling stage restrains the shrinkage of center element. Larger tensile stress results in stronger resistance against the shrinkage and smaller inherent strain. On the other hand, the compressive stress accelerates the shrinkage and the inherent strain increases.

This explanation can be extended to a plate model with an internal stress gradient at cooling stage through the thickness. Since the maximum welding temperature decreases through the thickness, the inherent strain (or stress) obtained from the inherent strain model of Fig. 16 becomes smaller as depicted in Fig. 18. The internal strain causes the shrinkage of heat affected zone and the decreasing shrinkage through the thickness results in the angular distortion.

The bending stress caused by the normal force applied on the side of plate is added to the internal force as shown in Fig. 18. Tensile and compressive forces occur on top surface and bottom surface of the plate, respectively. The inherent strain on the upper side increases while that in the lower side decreases. Consequentially, the slope of the inherent residual compressive force in weld during cooling through the thickness becomes less steep with reducing the angular distortion.

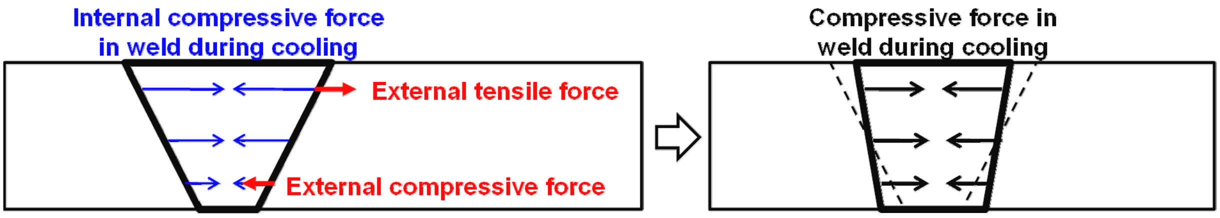

Fig. 18 Mechanism of restraint degree regarding external force during cooling.

COMPARISON OF WELDING ANALYSIS CONSIDERING EXTERNAL CONSTRAINT DURING COOLING STAGE

This section verifies the proposed inherent strain methods by comparing the results with EPA in terms of welding deformation and welding residual stress.

Analysis considering various external forces

Analyses of three cases having different welding conditions are performed. One is carried out under the general condition without external constraint. The other two cases are performed under different vertical forces acting along the edge of the work piece during the cooling stage, as depicted in Fig. 19. Two different forces induce two kinds of transverse bending stress; maximum values of 60, and 120 *MPa*. For each case, the welding distortions are calculated by two different methods; EPA and Improved ESM. The dimensions of the analysis model and welding conditions are listed in Table 2. The Gaussian-distributed heat source modeled is shown in Fig. 20 and used for a heat transfer analysis first.

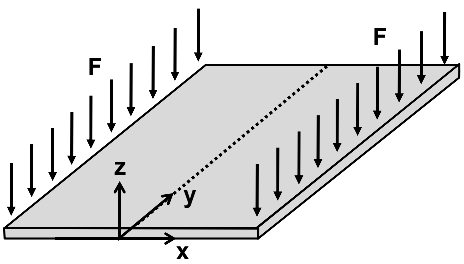

Fig. 19 Analysis case in which force is applied at both ends, perpendicular to weld line.

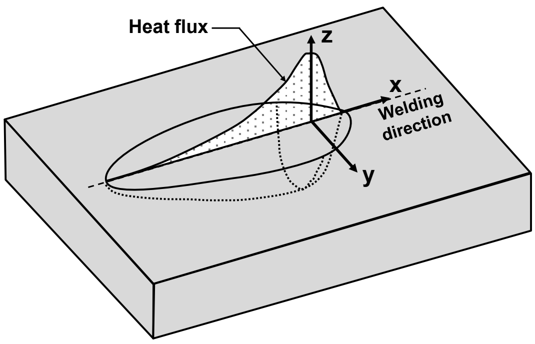

Fig. 20 Gaussian heat source model (Goldak et al., 1984).

Under the transient temperature distribution, EPA is performed. The maximum temperature at points around the heat affected zone are used for selecting the corresponding inherent strain values from the inherent strain chart of Fig. 17.

The analysis results for deformation are depicted in Figs. 21-23. The figures depict the deformation distribution of the model, and the graphs show vertical deformation on top surface along the transverse direction, which are measured at y=L/2.

Table 2 Dimensions and welding conditions of analysis model.

Dimensions		Welding conditions	
Length	500 *mm*	Voltage	30 *V*
Width	1000 *mm*	Current	300 *A*
Thickness	20 *mm*	Welding speed	0.01 *m/sec*

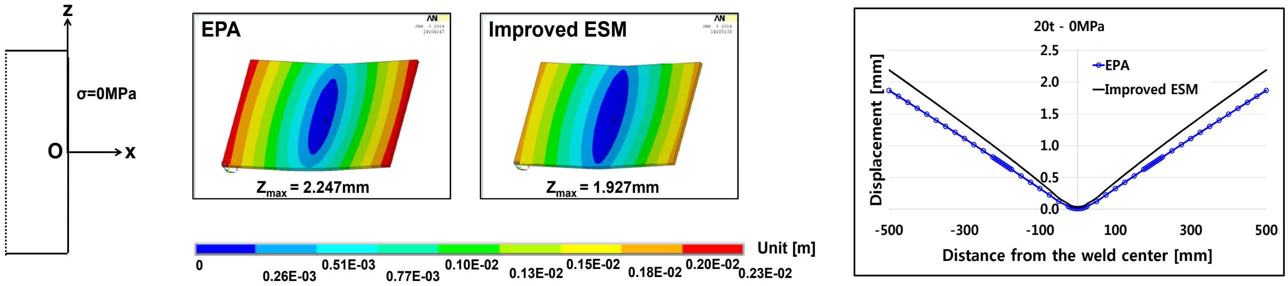

Fig. 21 Vertical deformation (max. bending stress of 0 *MPa*).

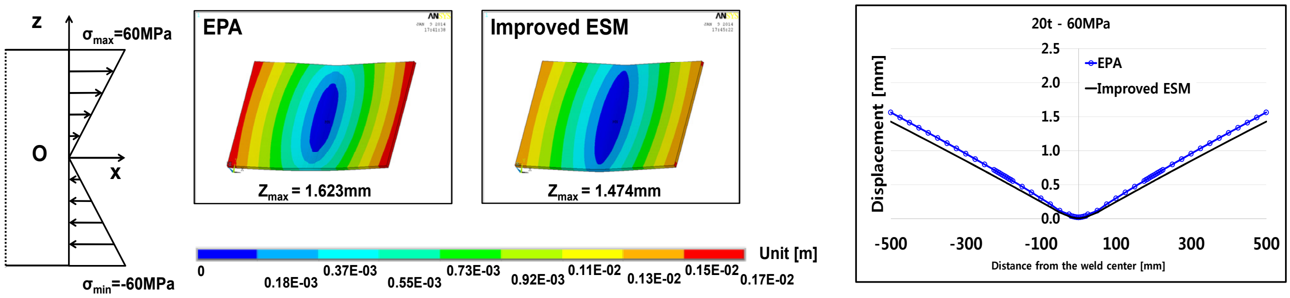

Fig. 22 Displacement in z direction (max. bending stress of 60 *MPa*).

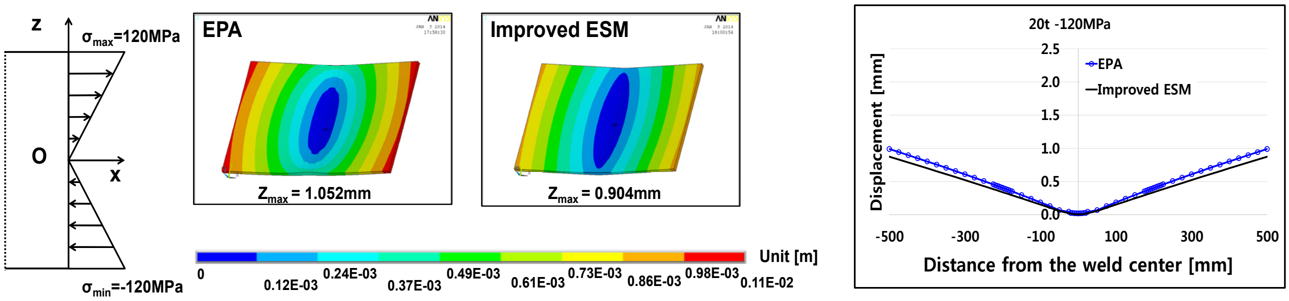

Fig. 23 Displacement in z direction (max. bending stress of 120 *MPa*).

The maximum vertical deformations at the edge of the plate are collected in Fig. 24. It can be seen that the deformation decreases as the external constraint force during cooling increases. The results of the EPA and Improved ESM show a difference of 14% on average.

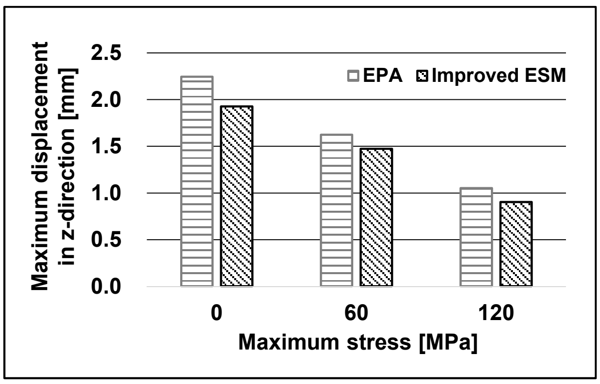

Fig. 24 Maximum displacement in z direction (applied bending stress 0 to 120 *MPa*).

Comparison of two external load cases (30 and 60 *MPa*) of equal bending moment

The following three different analysis methods are compared in this section for a validation of the introduction of equivalent bending moment.

EPA 1: Thermal elasto-plastic analyses with vertical load of F (1.69 *kN*) with 400 *mm* location.
EPA 2: Thermal elasto-plastic analyses with vertical load of 2F with 200 *mm* location.
Improved ISM: Improved equivalent strain analysis with the equivalent bending moment

The dimensions of the analysis model and welding conditions are listed in Table 3. The first two cases have the same bending moment at the center welding line and the resultant maximum bending stress on the top surface is calculated 30 *MPa* as follows.

$$F = 1.69kN$$

$$M = 0.4 \times F = 0.2 \times 2F = 674.68Nm$$

$$\sigma_{\max} = \frac{Mh}{2I} = 30MPa$$

Table 3 Dimensions and welding conditions of analysis model

Dimensions		Welding conditions	
Length	600 *mm*	Voltage	30 *V*
Width	800 *mm*	Current	300 *A*
Thickness	15 *mm*	Welding speed	0.01 *m/sec*

Figs. 25 and 26 show vertical welding deformation distribution and welding residual stress distributions in longitudinal direction on the top surface. Two graphs plot the deformation and the residual stress in the transverse direction at y=L/2 (at middle cross section).

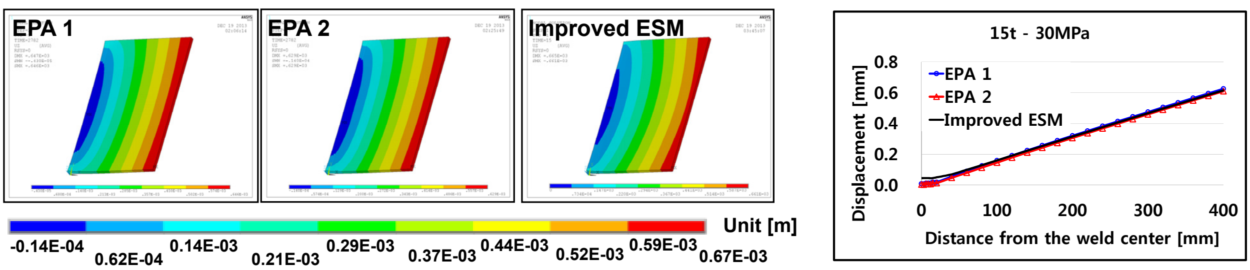

Fig. 25 Displacement in z direction (M).

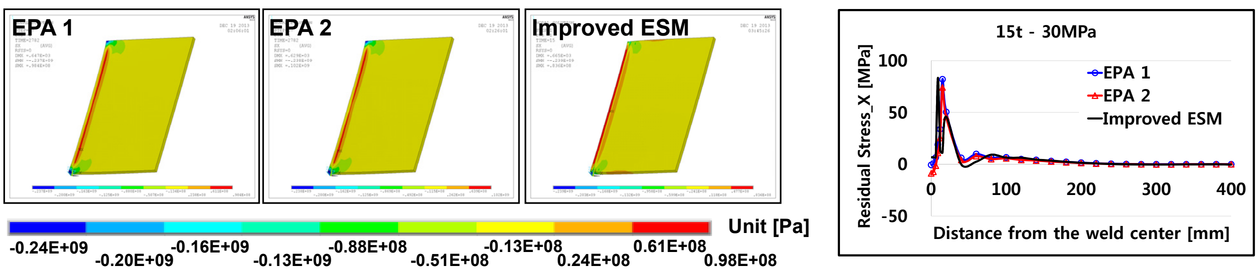

Fig. 26 Residual stress in x direction (M).

Another case study is performed with doubled external force, which corresponds to 60 *MPa* on the top surface along the welding line. The analysis results are shown in Figs. 27 and 28.

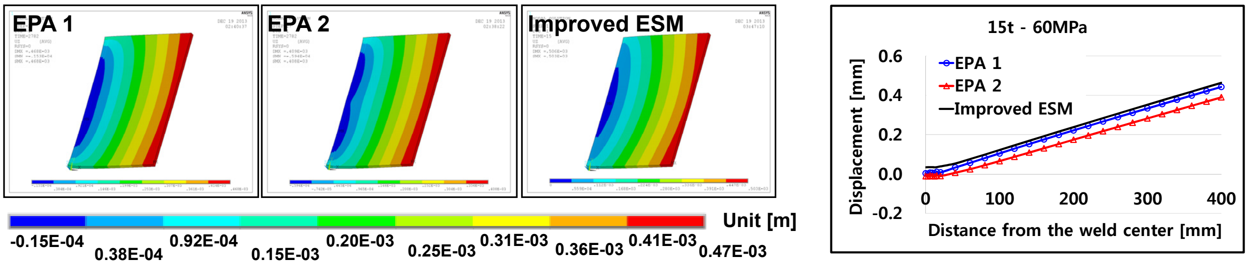

Fig. 27 Displacement in z direction (2M).

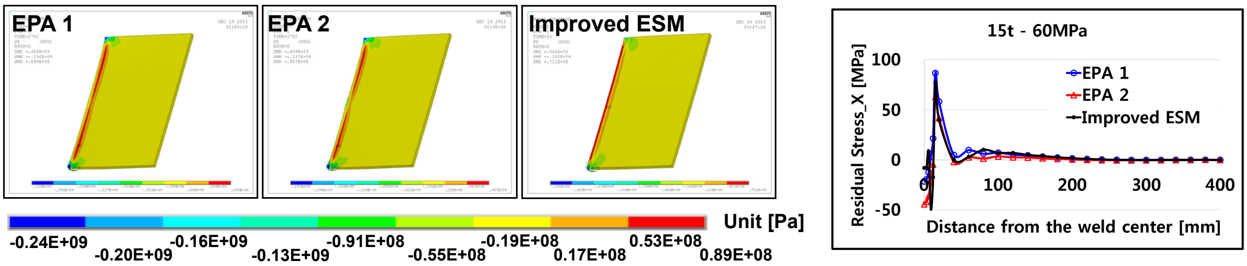

Fig. 28 Residual stress in x direction (2M).

The analysis results plotted in Fig. 29 proves that the deformation is reduced as the external constraint force during cooling increases. The results of the EPA and Improved ESM show a difference of 7% on average. It proves the validity of the proposed Improved ESM.

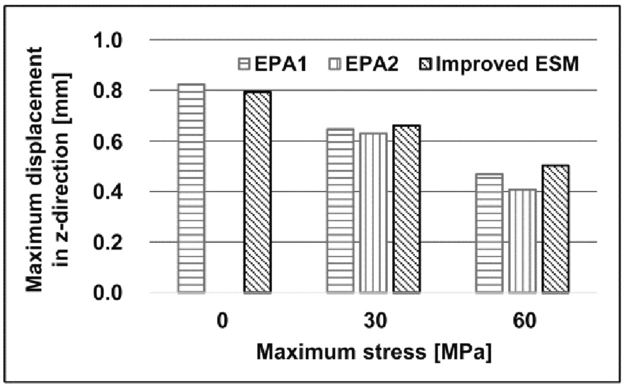

Fig. 29 Maximum displacement in z direction.

CONCLUSIONS

In the present study, the existing equivalent strain method was improved. This proposed method was verified by comparing the calculated welding deformation analysis results with those of a thermal elasto-plastic FE analysis. The main conclusions can be summarized as follows:

- External restraints imposed normal to the plate during the cooling stage are effective in reducing angular distortion.
- The welding analysis model under external force during the cooling stage is idealized as a prismatic member subjected to pure bending. The external restraint is represented by vertical force on both sides of the work piece, and bending stress forms

in the transverse direction. The additional bending stress distribution across the plate thickness is reflected in the improved inherent strain model.

- Improved ESM is adaptable for analysis of the welding model under external constraint during the cooling stage. Welding deformation can be calculated from an elastic linear FE analysis using the inherent strain values taken from the chart and compared with those from a 3D thermal elasto-plastic FE analysis.
- The proposed method is quick and accurate for welding analysis. This suggests its potential for application to large-scale structural analysis.

ACKNOWLEDGEMENT

This work was supported by the Technology Innovation Program, (10042556), Core Technology Development for Deepwater O&G Production System FEED Engineering & Floating Systems, funded by the Ministry of Trade, Industry & Energy (MI , Korea).

REFERENCES

Goldak, J., Chakravarti, A. and Bibby, M., 1984. A new finite element model for welding heat sources. *Metallurgical Transactions B*, 15(2), pp.299-305.

Jang, C.D., 2007. *Welding distortion analysis of hull blocks using equivalent load method based on inherent strain, Technical report SSC-453*. Washington, DC: Ship Structure Committee.

Kim, J.T., 2006. *Analysis of post weld deformation at HAZ by external forces based on inherent strain*. MS Thesis. Seoul National University.

Kim, T.J., Jang, B.S. and Kang, S.W., 2014. Welding deformation analysis based on improved equivalent strain method considering the effect of temperature gradients. *International Journal of Naval Architecture and Ocean Engineering*, 7(1), pp.157-173.

Kim, Y.T., 2010. *Structural analysis of ship hull block considering welding residual stress using equivalent strain method based on inherent strain*. Ph. D. Thesis. Seoul National University.

Lee, C.H., 2002. *Prediction of welding deformation of ship hull panel blocks using equivalent loading method based on inherent strain*. Ph. D. Thesis. Seoul National University.

Lee, D.W., 1995. *Thermo-elasto-plastic modeling of GMAW using the finite element method*. Ph. D. Thesis. Seoul National University.

Lee, J.H., 1999. *Relations between input parameters and residual deformations in line heating process using finite element method and multi-variate analysis*. Ph. D. Thesis. Seoul National University.

Radaj, D., 2003. *Welding residual stresses and distortion: calculation and measurement*. Sawston, Cambridge, UK: Woodhead Publishing Ltd.